

## Article

# Understanding the Role of *Trichoderma reesei* Vib1 in Gene Expression during Cellulose Degradation

Xiuzhen Chen <sup>1</sup>, Bingran Song <sup>1</sup>, Minglu Liu <sup>1</sup>, Lina Qin <sup>2</sup> and Zhiyang Dong <sup>1,\*</sup>

<sup>1</sup> State Key Laboratory of Microbial Resources, Institute of Microbiology, Chinese Academy of Sciences, Beijing 100101, China; chenxiuzhen@im.ac.cn (X.C.); songbingran16@mails.ucas.edu.cn (B.S.); liuminglu17@mails.ucas.ac.cn (M.L.)

<sup>2</sup> National and Local Joint Engineering Research Center of Industrial Microbiology and Fermentation Technology, College of Life Sciences, Fujian Normal University, Fuzhou 350117, China; qinln@fjnu.edu.cn

\* Correspondence: dongzy@im.ac.cn

**Abstract:** Vib1, a member of the Ndt80/PhoG-like transcription factor family, has been shown to be essential for cellulase production of *Trichoderma reesei*. Here, we combined transcriptomic and genetic analyses to gain mechanistic insights into the roles of Vib1 during cellulose degradation. Our transcriptome analysis showed that the *vib1* deletion caused 586 genes with decreased expression and 431 genes with increased expression on cellulose. The downregulated genes were enriched for Gene Ontology terms associated with carbohydrate metabolism, transmembrane transport, oxidoreductase activity, and transcription factor activity. Of the 258 genes induced by cellulose, 229 showed no or decreased expression in  $\Delta vib1$  on cellulose, including almost all (hemi)cellulase genes, crucial sugar transporter genes (IDs:69957, 3405), and the genes encoding main transcriptional activators Xyr1 and Ace3. Additionally, Vib1 also regulated the expression of genes involved in secondary metabolism. Further comparison of the transcriptomes of  $\Delta vib1$  and  $\Delta xyr1$  in cellulose revealed that the genes regulated by Vib1 had much overlap with Xyr1 targets especially for the gene set induced by cellulose, presumably whose expression requires the cooperativity between Vib1 and Xyr1. Genetic evidence indicated that Vib1 regulates cellulase gene expression partially via Xyr1. Our results will provide new clues for strain improvement.

**Keywords:** *Hypocrea jecorina*; lignocellulose; biomass; biorefinery; cellulase; transcription factor; secondary metabolism; transcriptome



**Citation:** Chen, X.; Song, B.; Liu, M.; Qin, L.; Dong, Z. Understanding the Role of *Trichoderma reesei* Vib1 in Gene Expression during Cellulose Degradation. *J. Fungi* **2021**, *7*, 613. <https://doi.org/10.3390/jof7080613>

Academic Editor: Javier Arroyo

Received: 7 July 2021

Accepted: 26 July 2021

Published: 29 July 2021

**Publisher's Note:** MDPI stays neutral with regard to jurisdictional claims in published maps and institutional affiliations.



**Copyright:** © 2021 by the authors. Licensee MDPI, Basel, Switzerland. This article is an open access article distributed under the terms and conditions of the Creative Commons Attribution (CC BY) license (<https://creativecommons.org/licenses/by/4.0/>).

## 1. Introduction

Lignocellulosic biomass is the most abundant source readily available that presents an enormous potential for the production of biofuels and other bio-based products [1]. Bioconversion of cellulose substrate into soluble sugars through cellulolytic enzymes represents a green, sustainable strategy for biorefinery [2,3]. The filamentous fungus *Trichoderma reesei* is one of the most extraordinary producers of cellulases and hemicellulases, and it has become a paradigm in breakdown of cellulosic biomass [4]. However, since the recalcitrance of lignocellulosic biomass to enzymatic hydrolysis leads to a requirement for large amounts of lignocellulolytic enzymes, the high cost of enzyme, which ranges from \$0.23 to \$0.78 per gallon of ethanol [5], is still a major bottleneck in lignocellulosic biofuel production [6,7]. Genetic engineering of *T. reesei* for enhanced enzyme production is an efficient approach to lower the contribution of enzymes to biofuel production costs. However, the progress is very slow due to our incomplete knowledge of the molecular mechanisms underlying cellulase expression. A better understanding of the regulatory network controlling cellulase production in *T. reesei* is imperative and would assist to develop new biotechnologies for cheaper production of cellulases.

The cellulase complex from *T. reesei* at least includes three types of synergistically acting enzymes: endoglucanases (EC 3.2.1.4), exoglucanases/cellobiohydrolases (EC 3.2.1.91),

and beta-glucosidases (EC 3.2.1.21), whose production is regulated mainly at the transcriptional level and obligatorily requires the presence of an inducer such as cellulose, disaccharides (cellobiose, sophorose) generated from cellulose degradation, or the soluble carbon source lactose. Additionally, most *T. reesei* cellulase genes are coordinately expressed [8,9], suggesting that a tight regulatory scheme operates in this fungus, which involves the fine-tuned cooperation of the respective transcription factors [10]. Several transcription factors are implicated in this process [11], including the positive master regulator Xyr1 [12] and the major carbon catabolite repressor Cre1 [13]. The last decade of investigation has revealed novel transcription factors for cellulase expression, including positive regulators Ace3 [14], Vel1 [15], BglR [16], Vib1 [17,18], and Azf1 [19], as well as the transcription repressor Rce1 [20]. Despite substantial advancements in identifying transcription factors, our knowledge is still incomplete about their roles during cellulase induction in *T. reesei*.

Vib1, a member of the Ndt80/PhoG-like transcription factor family that participates in the regulation of various metabolism processes, including meiosis [21], biofilm formation [22], and the response to nutrient stress [23], has recently been identified as a crucial regulator of cellulase production in *T. reesei* by two research groups with different means [17,18]. Vib-1, an orthologue of Vib1 in *Neurospora crassa*, is not only required for the expression of genes necessary for programmed cell death [24], but also essential for cellulose utilization [25]. It was proposed that the effect of *N. crassa* Vib-1 on cellulase production is achieved by inhibiting Cre1, and Col26, the BglR homologue of *N. crassa*, and inducing the positive master Clr-2 [25]. However, it is not clear which genes are subjected to regulation of the *T. reesei* Vib1 during cellulose degradation and the extent of overlap between the Vib1 regulon and the Xyr1 targets. In addition, it remains unknown whether Vib1 exerts its functions through Xyr1.

Here, to determine whether the requirement for *vib1* varies with the respective inducers, we investigated the cellulase production of the  $\Delta vib1$  mutant under different carbon sources. To define the extent of the Vib1 regulon, we performed RNA-seq to assess the genome-wide gene expression differences between parent strain and  $\Delta vib1$  grown on cellulose. In addition, to determine the genes regulated by Vib1 and Xyr1, we compared the transcriptomes of  $\Delta vib1$  and  $\Delta xyr1$  and mainly focused on analyzing the expression level of the Avicel regulon, the gene set that had higher expression on cellulose than under either glucose or no carbon source conditions. Moreover, we introduced an additional copy of constitutive *xyr1* expression cassette into  $\Delta vib1$  to test whether Vib1 exerts its functions through Xyr1.

## 2. Materials and Methods

### 2.1. Strains and Cultivation Conditions

*T. reesei* strains TU6 (ATCC MYA-256)  $\Delta tku70$ (TU6), TU6\_ $\Delta tku70\Delta vib1$ ( $\Delta vib1$ ), *vib1ce* (constitutive expression of *vib1* in  $\Delta vib1$ ), TU6\_ $\Delta tku70\Delta xyr1$ ( $\Delta xyr1$ ), and  $\Delta vib1::xyr1$  (constitutive expression of *xyr1* in  $\Delta vib1$ ) were cultivated on liquid minimal medium (MM) without peptone described previously [8], on a rotary shaker (250 rpm), at 28 °C. The pH of MM was adjusted to  $5.1 \pm 0.2$  with NaOH. Carbon sources were 1% (*w/v*), except that glucose was supplemented with 2% (*w/v*).

For replacement experiments [26], *T. reesei* strains were precultured in MM with glucose as sole carbon source for 30 h. Pre-grown mycelia were collected by gauze filtration and washed twice with carbon-free MM. Equal amounts of mycelia were transferred to flasks containing the appropriate carbon source (Avicel cellulose, lactose, cellobiose, and glucose) or no carbon source added and continued cultivation. At indicated time points, the cultures were sampled and centrifuged at 12,000 rpm, for 10 min, at 4 °C. The culture supernatants were then used for cellulase activity and protein concentration assays, whereas the harvested mycelia were used for biomass determination or total RNA isolation.

## 2.2. Enzyme Activity and Protein Concentration Assays

The filter paper hydrolyzing activity (FPase) and endo-beta-1,4-glucanase (CMCase) activity in culture supernatants were measured according to the International Union of Pure and Applied Chemistry (IUPAC) standard [27]. The extracellular protein concentration was determined by the Bradford method (Sangon Biotech Co., Ltd., Shanghai, China).

## 2.3. RNA Isolation, Library Preparation, RNA Sequencing

Mycelia were sampled at 8 h after shifting to MM containing Avicel cellulose, glucose, or no carbon source. Total RNA was extracted with TRIzol reagent (Invitrogen Life Technologies, Carlsbad, CA, USA), following the manufacturer's instructions. RNA integrity and purity were monitored on 1% agarose gels. Additional quality assessments were performed with the RNA Nano 6000 Assay Kit of the Bioanalyzer 2100 system (Agilent Technologies, Santa Clara, CA, USA) and the NanoPhotometer<sup>®</sup> spectrophotometer (IMPLEN, Los Angeles, CA, USA). RNA concentration was measured by using a Qubit<sup>®</sup> RNA Assay Kit in a Qubit<sup>®</sup> 2.0 Fluorometer (Life Technologies, Carlsbad, CA, USA).

The libraries were generated by using the NEBNext<sup>®</sup> Ultra<sup>™</sup> RNA Library Prep Kit for Illumina<sup>®</sup>, following the manufacturer's recommendations, and subjected to sequencing on an Illumina HiSeq platform with paired-end reads. The RNA-seq raw data are available at the SRA web site (<https://www.ncbi.nlm.nih.gov/sra>, accessed on 28 March 2021), under accession number SRP312496.

## 2.4. RNA-Seq Data Analysis

Clean data were obtained by removing reads containing adapter, poly-N and low-quality reads from raw data through in-house Perl scripts. Then the clean reads were mapped to the transcripts from the reference genome (<https://genome.jgi.doe.gov/Trire2/Trire2.home.html>, accessed on 26 January 2018), using Hisat2 v2.0.4. HTSeq v0.9.1 was used to count the reads numbers mapped to each gene and calculate FPKM (expected number of fragments per kilobase of transcript sequence per millions base pairs sequenced) [28]. Differential expression analysis of two conditions or groups was performed with the DESeq R package (1.18.0), with read counts as inputs. Genes with an adjusted  $p$ -value  $< 0.05$  and  $|\log_2\text{fold change}| \geq 1$  were assigned as differentially expressed. Gene Ontology (GO) enrichment analysis of differentially expressed genes was implemented by the Goseq R package, in which gene length bias was corrected. GO terms with corrected  $p$ -value less than 0.05 were considered significantly enriched by differentially expressed genes.

## 2.5. Real-Time Quantitative PCR (RT-qPCR)

DNase I-treated total RNA was used to synthesize first-strand cDNA according to the Invitrogen Superscript III first-strand synthesis kit. Except for *rpl6e*, which was used as a reference gene [29], RT-qPCR assays were performed as described by Chen et al. [30].

## 2.6. Construction of the *T. reesei* Mutants

For the recyclable use of the marker gene *pyr4* (ID 74020), a 3.7 kb *pyr4* blaster cassette with a loopout fragment was constructed as described [31]. In brief, the primer pairs Fpyr4-DR/Rpyr4-DR and Fpyr4/Rpyr4 were designed to amplify direct repeats (1.0 kb upstream of the *pyr4* start codon) and 2.3 kb of the *pyr4* expression cassette that consisted of direct repeats, *pyr4* coding regions, and *pyr4* terminators, respectively. The two purified PCR products were digested with *HindIII*/*NdeI* and *NdeI*/*BamHI* and ligated with *HindIII*/*BamHI*-digested pBluescript SK-plus (Stratagene), resulting in the pPYR4 plasmid. The 3.7 kb *pyr4* blaster cassette was released through the digestion of plasmid pPYR4 with *HindIII*/*BamHI* and used for subsequent plasmid construction.

The  $\Delta$ *vib1* mutant was generated by electroporating the uridine auxotrophic strain TU6\_ $\Delta$ *tku70* with the *vib1* gene deletion cassette, which contains 1.8 kb of 5' and 3' flanking regions of the open reading frame of *vib1* and a 3.7 kb of *pyr4* blaster cassette. The  $\Delta$ *xyr1*

mutant was obtained in the same manner, except that the 5' and 3' flanking regions of the *xyr1* gene were employed.

The *vib1ce* strain, in which *vib1* was constitutively expressed in  $\Delta$ *vib1*, was constructed by transforming the uridine auxotrophy strain  $\Delta$ *vib1* with a DNA fragment containing *A. nidulans* glyceraldehyde-3-phosphate dehydrogenase (GenBank: M33539.1) promoter, the open reading frame and terminator region of the *vib1* gene, and 2.7 kb *pyr4* expression cassette and 1.8 kb of sequence downstream of the *pyr4* stop codon used as homologous arms for targeted integration in the *pyr4* locus. The *xyr1* expression cassette targeting the *pyr4* locus was constructed in the same way, except that the coding and terminator regions of *xyr1* gene were used. The *xyr1* expression cassette was transformed into  $\Delta$ *vib1* to obtain  $\Delta$ *vib1::xyr1* strain.

The protocol for electroporation of *T. reesei* was performed according to the method described by Schuster et al. [29], except that a BIO-RAD Gene Pulser Xcell electroporation system was used in our study. The PCR method was used to confirm targeted integration of gene deletion or expression cassettes [32]. The copy number of the cassette integrated in the genome was determined by quantitative real-time PCR on the genomic DNA, as previously described [33].

All primers used in this study are listed in Supplementary Materials Table S1.

### 3. Results

#### 3.1. *Vib1* Is Required for Cellulolytic Enzyme Production Independent of Carbon Sources

The *vib1* deletion mutant ( $\Delta$ *vib1*) failed to provoke cellulase formation under cultivation conditions supplemented with a mixture of Solka-Floc cellulose and lactose as carbon sources [17]. We wondered whether the *vib1* deletion causes differential responses to the respective inducers; thus, we investigated the cellulase production of the  $\Delta$ *vib1* mutant under liquid MM with crystalline cellulose (Avicel PH-101, Sigma-Aldrich, St. Louis, MI, USA), lactose, or cellobiose as the sole carbon source. Irrespective of inducer strengths,  $\Delta$ *vib1* failed to produce extracellular protein on Avicel, lactose, or cellobiose (Figure 1), which is consistent with the results that almost no cellulase activity indicated by filter paper activity and CMCase activity was detected in strains lacking *vib1* (Figure 1). The  $\Delta$ *vib1* mutant showed defect growth on Avicel but not on lactose and cellobiose (Supplementary Materials Figure S1). The ectopic integration of a copy of *vib1* expression cassette driven by glyceraldehyde-3-phosphate dehydrogenase promoter from *Aspergillus nidulans* completely restored the growth of the  $\Delta$ *vib1* mutant on Avicel, extracellular protein production, and cellulase activity.

#### 3.2. Comparative Transcriptome Analysis of Parent Strain and the $\Delta$ *vib1* Mutant

To comprehensively understand the exact role of Vib1 in cellulose degradation, we utilized next-generation RNA sequencing to profile genome-wide mRNA abundances when the  $\Delta$ *vib1* mutant and parent strain were shifted to Avicel, glucose, or carbon-free medium for 8 h, following 30 h of pre-cultivation in glucose. RNA samples of three biological replicates from each condition were used for library preparation and sequencing, resulting in 15 sets of RNA-seq data. The data from three replicates of each condition showed a high Pearson correlation (Supplementary Materials Data S1).

For the parent strain, a comparative transcriptional profiling analysis between Avicel and no carbon source showed that 707 genes were differentially expressed, including 371 genes upregulated and 336 genes downregulated upon exposure to Avicel (Supplementary Materials Data S2). Only in the 371 upregulated gene set, there were enriched GO terms associated with hydrolase activity (corrected *p*-value:  $1.33 \times 10^{-17}$ ), carbohydrate metabolism (corrected *p*-value:  $1.15 \times 10^{-15}$ ), cellulose binding (corrected *p*-value:  $1.14 \times 10^{-7}$ ), and polysaccharide binding (corrected *p*-value:  $7.48 \times 10^{-7}$ ) (Supplementary Materials Figure S2). Of the 371 genes highly expressed on Avicel, 258 genes accumulated much more transcripts on Avicel than on glucose or no carbon (Supplementary Materials Figure S3), which were assigned as the "Avicel regulon" (Supplementary Materials Data S2).

The Avicel regulon contained 18 genes involved in cellulose degradation, including major cellulase genes and nonenzymatic cellulose attacking protein encoding genes; 23 characterized or predicted hemicellulase genes; 14 genes encoding predicted proteins with signal peptides. Additionally, included in the Avicel regulon were 22 genes encoding sugar transporters, including recently identified lactose permease Ctr1 (ID 3405) [32,34], mannose/cellobiose/xylose transporter (ID 69957) [35]. Additionally, the genes especially induced by cellulose contained 16 transcription factors, including Xyr1, Ace3, AmyR, and *N. crassa* cellulase regulator Clr-2 orthologue (IDs: 122208, 77513, 55105 and 26163). Genes involved in protein folding and modification were also included in the Avicel regulon. According to our conservative differential expression analysis (adjusted *p*-value < 0.05 and  $|\text{Log}_2\text{fold change}| \geq 1$ ), *vib1* (ID 54675) was not grouped into the Avicel regulon, but the mRNA level of *vib1* was relatively higher on Avicel than either on no-carbon or glucose conditions.

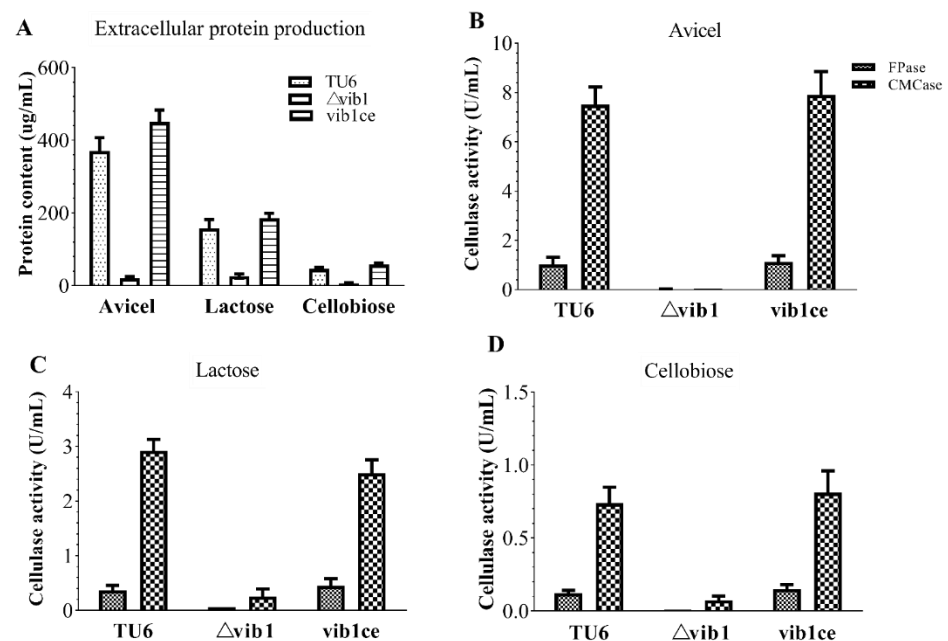


**Figure 1.** The effect of Vib1 on extracellular protein production and cellulase activity under different carbon sources. Parent strain TU6 and the *vib1* deletion mutant ( $\Delta vib1$ ), together with the *vib1* constitutive expression strain (*vib1ce*), were precultured in glucose-containing MM for 30 h; thereafter, the pre-grown mycelia were equally shifted to MM with Avicel cellulose, lactose, or cellobiose as the sole carbon source and continued cultivation for 120 h. The supernatants were collected for measuring extracellular protein content (A) and the volumetric cellulase activity (B–D). The values were means from three biological replicates. Error bars denoted standard deviations.

To gain insights into the extent to which Vib1 affects gene expression on Avicel, we compared the transcriptomes of the *vib1* deletion and parent strains under Avicel cultivation condition, and the expression of the abovementioned 707 differentially expressed genes in  $\Delta vib1$  on Avicel vs. on no carbon. The absence of *vib1* caused downregulation of 586 genes and upregulation of 431 genes in relative to parent strain on Avicel (Figure 2 and Supplementary Materials Data S3). The downregulated 586 genes were named as the “Vib1-dependent gene set”, which was enriched in functional categories, such as carbohydrate metabolism (corrected *p*-value:  $1.36 \times 10^{-23}$ ), transmembrane transport (corrected *p*-value:  $5.58 \times 10^{-19}$ ), hydrolase activity acting on glycosyl bonds (corrected *p*-value:  $6.30 \times 10^{-29}$ ), oxidoreductase activity (corrected *p*-value:  $4.27 \times 10^{-16}$ ), and RNA polymerase II transcription factor activity (corrected *p*-value:  $7.15 \times 10^{-9}$ ) (Supplementary Materials Figure S4A). For the upregulated genes, the most enriched functional categories were single-organism metabolic process (corrected *p*-value:  $1.47 \times 10^{-5}$ ), oxidation-reduction process (corrected



$p$ -value:  $4.96 \times 10^{-10}$ ), and transmembrane transport (corrected  $p$ -value:  $2.86 \times 10^{-5}$ ) (Supplementary Materials Figure S4B). For the 707 genes differentially expressed on Avicel and no carbon in the parent strain, the  $\Delta vib1$  mutant on Avicel showed almost the same expression profile as that on the no-carbon source (Figure 2 and Supplementary Materials Data S2), indicating that the  $\Delta vib1$  mutant failed to respond to the presence of cellulose in the environment, which supports the notion that sensing and responding to nutritional status is one of the ancestral roles for the Ndt80 family members [23].

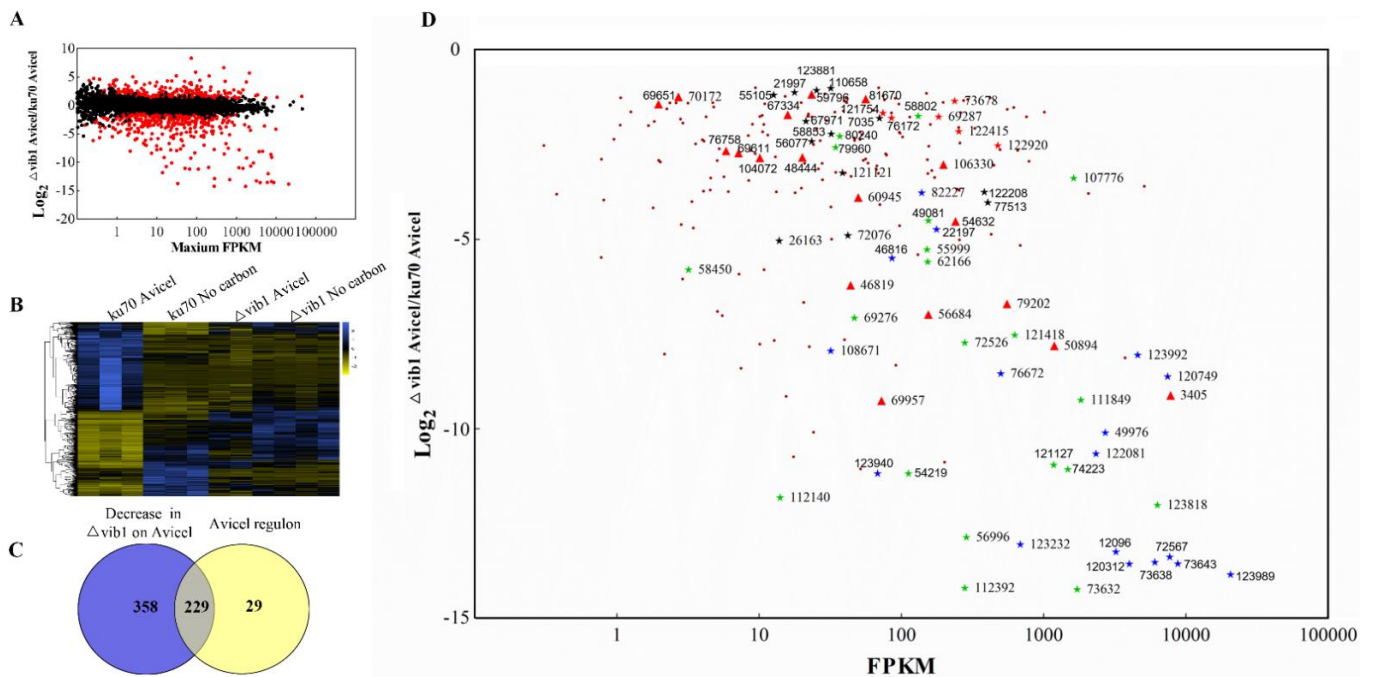


**Figure 2.** Transcriptional response of the  $\Delta vib1$  mutant to cellulose induction. (A) Genome-wide analysis of the influence of VibB1 on the transcriptomes of *T. reesei* on Avicel.  $\text{Log}_2$  ratio of  $\Delta vib1$ /TU6 on Avicel vs. maximum FPKM in either condition. Genes exhibiting differential expression ( $|\text{Log}_2\text{fold change}| \geq 1$  and adjusted  $p$ -value  $< 0.05$ ) are indicated with a red dot. (B) Hierarchical clustering of expression levels in  $\Delta vib1$  and TU6 for 707 genes differentially expressed in TU6 on Avicel cellulose and no carbon. Data from three biological replicates were included, and the expression level of gene was indicated with  $\text{log}_{10}$  FPKM. (C) Venn diagram of genes downregulated in the  $\Delta vib1$  mutant on Avicel cellulose compared to the Avicel regulon. (D) Fold change and expression level of the gene set within the Avicel regulon whose expression was downregulated in  $\Delta vib1$  on Avicel cellulose.  $\text{Log}_2$  ratio of  $\Delta vib1$ /TU6 read-count vs. FPKM in TU6 on Avicel was plotted. Genes encoding cellulase (★), hemicellulase (★), transcriptional factor (★), sugar transporter (▲), and secretory pathway component (★) are labeled with protein ID and indicated by the different symbols and colors. The other genes are indicated by red dot (•).

### 3.3. Analyses of the Vib1-Regulated Genes

Of the 586 Vib1-dependent genes, about 89% (229 genes) of the Avicel regulon showed no or reduced gene expression on Avicel in  $\Delta vib1$  when compared to parent strain (Figure 2 and Supplementary Materials Data S3), which comprise almost all (hemi)cellulose-degrading genes except *cel3e* within the Avicel regulon and 18 sugar transporter genes, including ID 69957 and ID 3405. Additionally, 13 out of 16 transcription-factor-encoding genes in the Avicel regulon were significantly downregulated in the  $\Delta vib1$  mutant, including *xyr1*, *ace3*, *amyr*, and the *N. crassa clr-2* orthologue (Figure 2). Vib1 also had positive effects on the transcriptional levels of genes involved in protein folding and modification (IDs: 122415, 122920, 60085, and 73678). The remaining 29 genes within the Avicel regulon mainly encode hypothetical proteins. These data indicated that Vib1 is a crucial regulator of the Avicel regulon in *T. reesei*. Besides the Avicel regulon, Vib1 also influenced the expression levels of genes encoding the transcription factors AreA (ID: 76817) and the

*N. crassa* Clr-1 orthologue (ID: 27600). It shall be noted that reduced expression of *cre1* ( $\log_2$ fold change =  $-0.91818$ ,  $p = 0.023$ ) was observed in  $\Delta vib1$ .

Our transcriptome analysis also pointed to a regulatory role of Vib1 in secondary metabolism. Sorbicillin, a typical yellow pigment secreted by fungi, including *Trichoderma* [36–38], is a hexaketide secondary metabolite with diverse bioactivities [39,40]. The sorbicillin (SOR) gene cluster comprises two polyketide synthases, Pks11/Sor1 (ID 73618) and Pks10/Sor2 (ID: 73621); two auxiliary modifiers (IDs: 73623 and 73631); one transporter (ID: 43701); and two yellow pigment regulators, Ypr1 and Ypr2 (IDs: 102499 and 102497) [36,41]. Our results showed that all genes within the SOR cluster displayed enhanced transcript accumulation on Avicel in  $\Delta vib1$  (Table 1), with *sor3* having the highest fold change ( $\log_2$ fold change = 8.3199). Besides the SOR gene cluster, Vib1 also affected the expression of three polyketide synthase genes (IDs: 65172, 82208, and 59482), four non-ribosomal peptide synthase (NRPS) genes (IDs: 81014, 123786, 68204, and 69946), and one NRPS/PKS fusion gene (ID: 58285). Additionally, Vib1 negatively regulated the expression level of the transcription factor Vel1, a regulator of cellulase gene expression, development, and secondary metabolism biosynthesis [15].

**Table 1.** Vib1 affects the expression of the SOR cluster and other secondary metabolism-associated genes on Avicel.

| Description                            | Protein ID | $\log_2 (\Delta vib1/TU6)$ | Adjusted <i>p</i> -Value |
|--|------------|----------------------------|--------------------------|
| Polyketide synthase Pks11S/Sor1        | 73618      | 4.324                      | $1.89 \times 10^{-19}$   |
| Polyketide synthase Pks10S/Sor2        | 73621      | 3.941                      | $1.46 \times 10^{-11}$   |
| FAD-dependent monooxygenase Sor3       | 73623      | 8.320                      | $3.04 \times 10^{-10}$   |
| FAD/FMN-containing dehydrogenase/Sor4  | 73631      | 1.844                      | 0.0021573                |
| MFS multidrug-resistance transporter   | 43701      | 4.243                      | $1.36 \times 10^{-33}$   |
| Transcription factor Ypr1              | 102499     | 2.513                      | 0.00012598               |
| Transcription factor Ypr2              | 102497     | 2.788                      | $6.22 \times 10^{-16}$   |
| Polyketide synthase Pks1               | 65172      | 2.773                      | 0.01383                  |
| Polyketide synthase Pks4               | 82208      | $-2.448$                   | 0.013456                 |
| Polyketide synthase Pks5               | 59482      | $-1.770$                   | $6.83 \times 10^{-7}$    |
| Non-ribosomal peptide synthases (NRPS) | 81014      | $-1.154$                   | 0.03429                  |
| Non-ribosomal peptide synthases (NRPS) | 123786     | $-1.192$                   | 0.0049844                |
| Non-ribosomal peptide synthases (NRPS) | 68204      | $-1.801$                   | $2.8 \times 10^{-7}$     |
| Non-ribosomal peptide synthases (NRPS) | 69946      | $-1.449$                   | $6.04 \times 10^{-5}$    |
| NRPS/PKS hybrid                        | 58285      | 1.449                      | 0.0011556                |
| Transcription factor Vel1              | 122284     | 1.473                      | $3.32 \times 10^{-5}$    |

### 3.4. The Vib1-Dependent Gene Set Considerably Overlaps with Xyr1 Targets

For cellulase and extracellular protein production on cellulose, Vib1 demonstrated almost the same output as the cellulase transcriptional regulator Xyr1, suggesting that Vib1 may share regulatory targets with Xyr1. To test this hypothesis, we also performed transcriptome sequencing of the  $\Delta xyr1$  mutant on cellulose in parallel with the  $\Delta vib1$  mutant and parent strain. The deletion of *xyr1* caused 2064 genes differentially expressed when compared with parent strain on Avicel, including 1218 downregulated genes and 846 upregulated genes (Supplementary Materials Data S4). The Vib1-dependent 586-gene set overlapped with Xyr1 targets by 371 genes. Of the 229 genes within the Avicel regulon which were downregulated in  $\Delta vib1$ , 211 genes showed decreased or no expression in  $\Delta xyr1$  on Avicel (Figure 3).

The overlapped 211 genes included almost all (hemi)cellulose-degrading genes, except for *cel3e*, within the Avicel regulon; 14 sugar transporter genes, including ID 69957 and ID 3405; and 11 (putative) transcription factor-encoding genes, including *ace3* and *thecr-2* homologue (Table 2). Genes involved in posttranslational modification, intracellular trafficking, and secretion (e.g., ER chaperone Bip1, protein disulfide isomerase Pdi1, DnaJ superfamily molecular chaperone, COPII vesicle protein, ER-resident chaperone calnexin, alpha-1,2-mannosidase, alpha-mannosyltransferase, glucosidase II catalytic (alpha) sub-

unit GII, and secretory pathway protein Ysy6) (Supplementary Materials Table S3) were also regulated in common by Vib1 and Xyr1. Of note, over 50% of 211 genes were affected by Vib1 and Xyr1 to a similar degree, suggesting that the cooperativity between Vib1 and Xyr1 might be required for the expression of these genes.

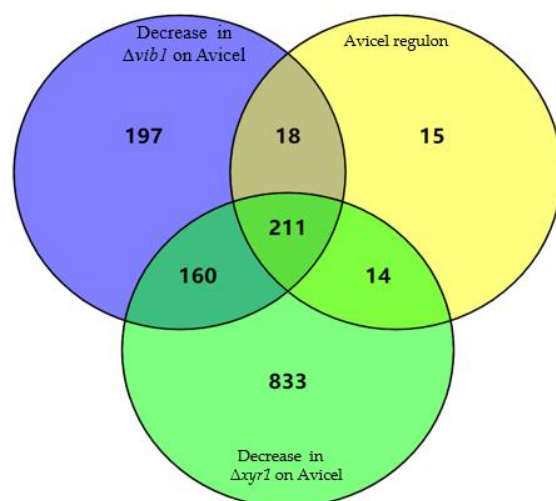


**Figure 3.** Venn diagram of genes downregulated in  $\Delta vib1$  and  $\Delta xyr1$  on Avicel compared to the Avicel regulon.

**Table 2.** Fold change of genes encoding cellulase, hemicellulase, sugar transporter, and transcription factor of the Avicel regulon in  $\Delta vib1$  and  $\Delta xyr1$  on Avicel.

| Category | Description                           | Protein ID | Log <sub>2</sub> ( $\Delta vib1$ /TU6) | Log <sub>2</sub> ( $\Delta xyr1$ /TU6) |
|----------|---------------------------------------|------------|--|--|
|          | Cellulase                             |            |  |  |
|          | Endo-beta-1,4-glucanase Egl2/Cel5a    | 120312     | −13.571                                | −13.839                                |
|          | Endo-beta-1,4-glucanase Egl4/Cel61a   | 73643      | −13.566                                | −13.757                                |
|          | Cellulose-binding protein Cip1        | 73638      | −13.531                                | −13.627                                |
|          | Cellobiohydrolase I CBHI/Cel7a        | 123989     | −13.850                                | −13.508                                |
|          | Cellobiohydrolase II CBHII/Cel6a      | 72567      | −13.386                                | −13.504                                |
|          | Endo-beta-1,4-glucanase Egl4/Cel61b   | 120961     | −13.254                                | −13.140                                |
|          | Endo-beta-1,4-glucanase Egl3/Cel12a   | 123232     | −13.059                                | −12.674                                |
|          | Endo-beta-1,4-glucanase Egl1/Cel7b    | 122081     | −10.661                                | −11.889                                |
|          | Endo-beta-1,4-glucanase Egl5/Cel45a   | 49976      | −10.107                                | −10.585                                |
|          | Cellulose-binding protein Cip2        | 123940     | −11.185                                | −10.497                                |
|          | Non-catalytic module family expansion | 123992     | −8.059                                 | −9.543                                 |
|          | Beta-glucosidase Bgl1/Cel3a           | 76672      | −8.548                                 | −8.500                                 |
|          | Beta-glucosidase Bgl2/Cel1a           | 120749     | −8.625                                 | −8.165                                 |
|          | Cand Beta-glucosidase Bgl3f           | 108671     | −7.950                                 | −7.413                                 |
|          | Beta-glucosidase Cel3d                | 46816      | −5.502                                 | −6.768                                 |
|          | Cand Beta-glucosidase Cel1b           | 22197      | −4.737                                 | −4.342                                 |
|          | Beta-glucosidase Cel3c                | 82227      | −3.772                                 | −3.146                                 |
|          | Hemicellulase                         |            |  |  |
|          | Beta-galactosidase Bga1               | 80240      | −2.282                                 | −2.036                                 |
|          | Endo-beta-1,4-xylanase Xyn1           | 74223      | −11.073                                | −15.128                                |
|          | Cand endo-beta-1,4-xylanase Xyn5      | 112392     | −14.207                                | −14.367                                |
|          | Acetyl xylan esterase Axe1            | 73632      | −14.242                                | −14.178                                |
|          | Beta-xylosidase Bxl1                  | 121127     | −10.959                                | −12.475                                |
|          | Beta-mannanase Man1                   | 56996      | −12.868                                | −12.387                                |
|          | Endo-beta-1,4-xylanase Xyn2           | 123818     | −12.017                                | −12.201                                |
|          | Acetyl xylan esterase                 | 54219      | −11.187                                | −11.586                                |



Table 2. Cont.

| Category | Description  | Protein ID | Log2<br>( $\Delta vib1$ /TU6) | Log2<br>( $\Delta xyr1$ /TU6) |
|----------|--|------------|-------------------------------|-------------------------------|
|          | Endo-beta-1,4-xylanase Xyn4                        | 111849     | −9.243                        | −10.847                       |
|          | Alpha-glucuronidase Glr1                           | 72526      | −7.733                        | −10.480                       |
|          | Acetyl esterase Aes1                               | 121418     | −7.528                        | −9.969                        |
|          | Cand alpha-L-arabnofuranosidase Abf2               | 76210      | −7.841                        | −8.324                        |
|          | Endo-beta-1,4-xylanase Xyn3                        | 120229     | −7.677                        | −7.868                        |
|          | Cand.endo-beta 1,4-xylanase                        | 69276      | −7.079                        | −7.685                        |
|          | Cand exo-polygalacturonase                         | 112140     | −11.818                       | −7.545                        |
|          | Cand Beta-xylosidase Xyl3b                         | 58450      | −5.803                        | −6.661                        |
|          | Alpha-galactosidase                                | 55999      | −5.270                        | −6.167                        |
|          | NAD (P)H-dependent D-xylosereductase Xyl1          | 107776     | −3.387                        | −5.771                        |
|          | Beta-mannosidase                                   | 62166      | −5.597                        | −5.429                        |
|          | Cand.beta-xylosidase/alpha-L-arabinofuranosidase   | 3739       | −3.344                        | −4.965                        |
|          | Xyloglucanase Cel74a                               | 49081      | −4.508                        | −4.639                        |
|          | Cand endo-polygalacturonase                        | 103049     | −2.920                        | −3.504                        |
|          | Cand.endo-beta 1,6-galactanase                     | 110894     | −2.663                        | −3.022                        |
|          | Sugar transporter                                  |            |                               |                               |
|          | Mannose/cellobiose/xylose transporter              | 69957      | −9.266                        | −10.316                       |
|          | Lactose permease Crt1                              | 3405       | −9.124                        | −8.166                        |
|          | MFS permease                                       | 50894      | −7.813                        | −7.923                        |
|          | Putative mono- or disaccharide transporters        | 56684      | −6.986                        | −7.209                        |
|          | MFS permease                                       | 46819      | −6.216                        | −6.713                        |
|          | Putative mono- or disaccharide transporter         | 79202      | −6.707                        | −5.783                        |
|          | MFS permease                                       | 54632      | −4.525                        | −4.246                        |
|          | L-arabinose isomerase                              | 106330     | −3.025                        | −2.557                        |
|          | MFS permease                                       | 69611      | −2.721                        | −2.523                        |
|          | MFS maltose permease                               | 48444      | −2.834                        | −2.469                        |
|          | MFS permease, hexose transporter                   | 104072     | −2.850                        | −2.403                        |
|          | L-arabinose isomerase                              | 60945      | −3.894                        | −2.370                        |
|          | MFS maltose permease                               | 76758      | −2.664                        | −1.852                        |
|          | MFS L-fucose permease                              | 67334      | −1.709                        | −1.168                        |
|          | Transcription factor                               |            |                               |                               |
|          | Zn2Cys6 transcriptional regulator Xyr1             | 122208     | −3.757                        | −12.387                       |
|          | N-terminal binuclear Zn cluster-containing protein | 72076      | −4.898                        | −4.959                        |
|          | Zn2Cys6 transcriptional regulator Clr2             | 26163      | −5.037                        | −4.155                        |
|          | C2HC transcriptional regulator Ace3                | 77513      | −4.033                        | −3.737                        |
|          | Fungal transcriptional regulatory protein          | 121121     | −3.248                        | −2.913                        |
|          | Fungal transcriptional regulatory protein          | 56077      | −2.414                        | −2.662                        |
|          | N-terminal binuclear Zn cluster-containing protein | 123881     | −1.065                        | −1.817                        |
|          | ZF-MYND like protein                               | 67971      | −1.879                        | −1.775                        |
|          | Predicted protein Myb                              | 58853      | −2.220                        | −1.635                        |
|          | Zn2Cys6 transcriptional regulator                  | 70351      | −1.803                        | −1.513                        |
|          | Zn2Cys6 transcriptional regulator AmyR             | 55105      | −1.193                        | −1.030                        |

### 3.5. Constitutive Expression of *xyr1* Partially Restored the Cellulase Production Ability of the $\Delta vib1$ Mutant

The result that the *vib1* deletion significantly reduced the transcriptional level of *xyr1* on cellulose prompted us to ask whether Vib1 acts through Xyr1 to regulate cellulase gene expression. If Xyr1 is subjected to the direct control of Vib1, the constitutive expression of *xyr1* gene theoretically should bypass the requirement of Vib1. To test this hypothesis, we constructed strain  $\Delta vib1::xyr1$ , in which an additional copy of the *xyr1* constitutive expression cassette was integrated into the genome of  $\Delta vib1$ . As shown in Figure 4, constitutive expression of *xyr1* only partially restored the cellulolytic capacity of  $\Delta vib1$ ; however, the mRNA level of *xyr1* in the  $\Delta vib1::xyr1$  mutant was higher than that in parent strain. These results suggested that Vib1 acts at least in part via Xyr1 to regulate cellulase

biosynthesis; on the other hand, the exertion of the Xyr1 function likely depends on the involvement of Vib1 or other additional factors.

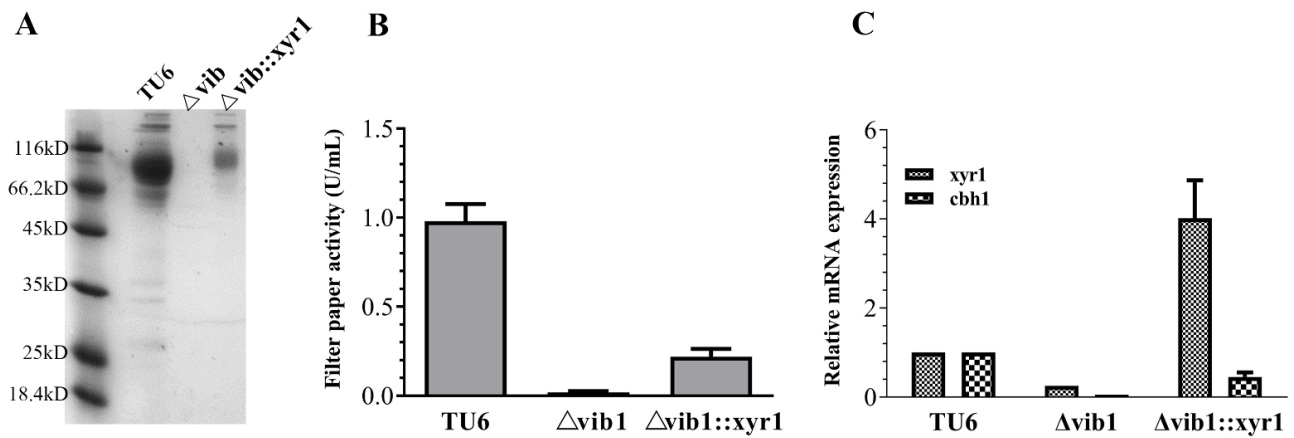


**Figure 4.** Constitutive expression of *xyr1* partially restored cellulase production of the  $\Delta vib1$  mutant on Avicel. The secretomes (A) and cellulase activity (B) of the culture supernatant in TU6,  $\Delta vib1$ , and  $\Delta vib1::xyr1$  120 h after transfer to Avicel cellulose from glucose. (C) RT-PCR measurement of *xyr1* and *cbh1* expression in TU6 versus  $\Delta vib1$  and  $\Delta vib1::xyr1$  24 h after transfer to Avicel cellulose from glucose. Expression level was normalized to the parent strain TU6.

#### 4. Discussion

In the present study, we demonstrated that the  $\Delta vib1$  mutant abolished cellulase production irrespective of inducer strength and displayed defect growth on Avicel but not on lactose and cellobiose. By RNA-seq, we analyzed the genes regulated by Vib1 under Avicel cultivation conditions and identified the core gene set commonly regulated by Vib1 and Xyr1. By genetic analysis, we showed that Vib1 controls cellulase expression partially via Xyr1.

Our transcriptome comparison between parent strain and  $\Delta vib1$  showed that the *vib1* deletion significantly reduced the expression level of *xyr1*, *ace3*, *cre1*, and the *N. crassa* *clr-1* and *clr-2* homologues, but exerted no effect on the mRNA level of *bglR* on Avicel. Similarly, the expression of *bglR* on lactose was also not affected by Vib1 [17]. This is different from the case in *N. crassa*, where functional loss of *N. crassa* Vib1 resulted in significantly reduced mRNA levels of the transcription factor Clr2 essential for cellulase induction [42] but increased transcriptional levels of the genes encoding carbon catabolite repressor Cre1 and the *T. reesei* BglR orthologue Col-26 critical for glucose sensing/metabolism [25]. The reason for this phenomenon is the difference of transcription machinery between *T. reesei* and *N. crassa* [43]. Therefore, despite functional conservation in cellulase production, the regulatory circuit of Vib1 was rewired in *T. reesei*.

Previous studies revealed that the transcription factor Ace3 is essential for the expression of cellulase genes [14], which governs cellulase activity through Xyr1 and the cellulose response transporter Crt1 [34]. Here, we showed that the deletion of *vib1* or *xyr1* significantly reduced the transcript accumulation of *ace3*. Meanwhile, Vib1 and Xyr1 positively regulated each other irrespective of the extent. Additionally, by analyzing the gene expression pattern of the Avicel regulon in  $\Delta vib1$  and  $\Delta xyr1$  on cellulose, we found that there was considerable overlap between the genes regulated by Vib1 and Xyr1. Taken together, it is possible that Vib1, Xyr1, and Ace3 constitute a core regulatory circuit and may depend on each other to achieve individual functions. Alternatively, the effect of Vib1 on cellulase expression may be achieved through activating Ace3, thus facilitating the interaction of Ace3 with Xyr1 or other factors.

There are several lines of evidence pointing to the crosstalk between plant cell wall deconstruction enzyme expression and secondary metabolism biosynthesis in *T. reesei* [37,44–48], which involves methyltransferase Lae1, YPK1-type kinase Usk1, catalytic subunit of protein kinase A (PKAc1), and transcription factors (Vel1, Cre1, Xpp1, and Ypr2). It has been

demonstrated that Cre1, Usk1, PKAc1, and Xpp1 control the expression of the SOR cluster, including the transcription factors Ypr1 and Ypr2 [37,45,47,48]. Our results indicated that, besides cellulase biosynthesis, Vib1 controls the expression of the SOR gene cluster; however, Vib1 had no effect on the mRNA levels of Usk1, PKAc1, and Xpp1, indicating that Vib1 might act downstream of the three regulators. This requires further investigation. In addition to the SOR cluster, we found that VIB1 also regulated the expression of three PKS genes, four NRPS genes, one NRPS/PKS fusion gene, and the global secondary metabolism regulator Vel1. These findings suggest that Vib1 might exert a broad influence on secondary metabolism in *T. reesei*.

## 5. Conclusions

This study showed that Vib1 was involved in cellulose degradation through the control of multiple gene expression beyond carbohydrate metabolism. The set of 586 Vib1-dependent genes overlapped with Xyr1 targets by 371 genes, including 211 genes within the Avicel regulon. The overlapped 211 genes included almost all (hemi)cellulose-degrading genes, except for cel3e; and characterized crucial sugar transporter- and transcription factor-encoding genes, which may constitute the backbone of the whole cellulose degradation system. We propose that their expression may be dependent on the cooperativity between Vib1 and Xyr1. The result that constitutive expression of *xyr1* only partially restored the cellulase production ability of the  $\Delta vib1$  mutant, to some extent, showed that the implementation of the Xyr1 function required the involvement. Further research is needed to test this hypothesis. Taken together, the present work has revealed new aspects of cellulase expression regulation in *T. reesei*. Such knowledge has important implications for the improvement of cellulase production by *T. reesei*.

**Supplementary Materials:** The following are available online at <https://www.mdpi.com/article/10.3390/jof7080613/s1>. Figure S1: Mycelial biomass accumulation of the *vib1* deletion strain TU6\_ $\Delta tku70\Delta vib1$  ( $\Delta vib1$ ) relative to the parent strain TU6\_ $\Delta tku70$  (TU6) and the *vib1* constitutive expression strain *vib1ce*. Figure S2: Genome-wide analysis of transcriptional induction by Avicel cellulose in *T. reesei*. Figure S3: Hierarchical cluster of expression levels in TU6 on glucose, no-carbon, and Avicel cellulose for 707 genes differentially expressed on Avicel cellulose and no carbon 8 h after transfer. Figure S4. Gene Ontology (GO) enrichment analysis of genes differentially expressed in  $\Delta vib1$  on Avicel as compared to TU6 on Avicel 8 h after transfer from glucose. The most enriched GO terms for downregulated genes (A) and upregulated genes (B) in the  $\Delta vib1$  mutant. The GO items with adjusted *p*-value < 0.05 are indicated with the symbol “\*”. Data S1: A summary of transcriptome data. Data S2: The 707 differentially expressed genes in TU6 exposed to Avicel in relative to no carbon and their expression level and fold change in  $\Delta vib1$ . Data S3: The genes regulated by VIB1. Data S4: Gene list regulated by XYR1 on Avicel. Table S1: Oligonucleotides used in this study.

**Author Contributions:** Conceptualization, X.C., L.Q. and Z.D.; methodology, X.C., B.S. and M.L.; software, X.C. and B.S., validation, X.C., B.S. and M.L.; formal analysis, X.C., L.Q. and Z.D.; investigation, X.C. and Z.D.; resources, Z.D.; data curation, X.C.; writing—original draft preparation, X.C.; writing—review and editing, X.C.; visualization, X.C. and Z.D.; supervision, Z.D.; project administration, Z.D.; funding acquisition, Z.D.; funding acquisition, Z.D. All authors have read and agreed to the published version of the manuscript.

**Funding:** This work was financially supported by the National Natural Science Foundation of China (30970073) and the National Key R&D Program of China (2018YFC0310703).

**Institutional Review Board Statement:** Not applicable.

**Informed Consent Statement:** Not applicable.

**Data Availability Statement:** The RNA-seq raw data are available at the SRA website (<https://www.ncbi.nlm.nih.gov/sra>, accessed on 28 March 2021) under accession number SRP312496.

**Acknowledgments:** We thank Linhuan Wu, Qinglan Sun, and Jingjing Yang (Institute of Microbiology, Chinese Academy of Sciences) for their assistance in submitting data.

**Conflicts of Interest:** The authors declare no conflict of interest.

## References

1. Fatma, S.; Hameed, A.; Noman, M.; Ahmed, T.; Shahid, M.; Tariq, M.; Sohail, I.; Tabassum, R. Lignocellulosic biomass: A sustainable bioenergy source for the future. *Protein Pept. Lett.* **2018**, *25*, 148–163. [[CrossRef](#)]
2. Kubicek, C.P. Systems biological approaches towards understanding cellulase production by *Trichoderma reesei*. *J. Biotechnol.* **2013**, *163*, 133–142. [[CrossRef](#)]
3. Soni, S.K.; Sharma, A.; Soni, R. Cellulases: Role in lignocellulosic biomass utilization. *Methods Mol. Biol.* **2018**, *1796*, 3–23. [[PubMed](#)]
4. Schmoll, M. The information highways of a biotechnological workhorse—Signal transduction in *Hypocrea jecorina*. *BMC Genom.* **2008**, *9*, 430. [[CrossRef](#)] [[PubMed](#)]
5. Johnson, E. Integrated enzyme production lowers the cost of cellulosic ethanol. *Biofuel. Bioprod. Bioref.* **2016**, *10*, 164–174. [[CrossRef](#)]
6. Klein-Marcuschamer, D.; Oleskowicz-Popiel, P.; Simmons, B.A.; Blanch, H.W. The challenge of enzyme cost in the production of lignocellulosic biofuels. *Biotechnol. Bioeng.* **2012**, *109*, 1083–1087. [[CrossRef](#)] [[PubMed](#)]
7. Adsul, M.; Sandhu, S.K.; Singhania, R.R.; Gupta, R.; Puri, S.K.; Mathur, A. Designing a cellulolytic enzyme cocktail for the efficient and economical conversion of lignocellulosic biomass to biofuels. *Enzyme Microb. Technol.* **2020**, *133*, 109442. [[CrossRef](#)]
8. Ilmén, M.; Saloheimo, A.; Onnela, M.L.; Penttilä, M.E. Regulation of cellulase gene expression in the filamentous fungus *Trichoderma reesei*. *Appl. Environ. Microbiol.* **1997**, *63*, 1298–1306. [[CrossRef](#)]
9. Foreman, P.K.; Brown, D.; Dankmeyer, L.; Dean, R.; Diener, S.; Dunn-Coleman, N.S.; Goedegebuur, F.; Houfek, T.D.; England, G.J.; Kelley, A.S.; et al. Transcriptional regulation of biomass-degrading enzymes in the filamentous fungus *Trichoderma reesei*. *J. Biol. Chem.* **2003**, *278*, 31988–31997. [[CrossRef](#)]
10. Portnoy, T.; Margeot, A.; Seidl-Seiboth, V.; Le Crom, S.; Ben Chaabane, F.; Linke, R.; Seiboth, B.; Kubicek, C.P. Differential regulation of the cellulase transcription factors XYR1, ACE2, and ACE1 in *Trichoderma reesei* strains producing high and low levels of cellulase. *Eukaryot Cell* **2011**, *10*, 262–271. [[CrossRef](#)]
11. Kubicek, C.P.; Mikus, M.; Schuster, A.; Schmoll, M.; Seiboth, B. Metabolic engineering strategies for the improvement of cellulase production by *Hypocrea jecorina*. *Biotechnol. Biofuels* **2009**, *2*, 19. [[CrossRef](#)] [[PubMed](#)]
12. Stricker, A.R.; Grosstessner-Hain, K.; Wurleitner, E.; Mach, R.L. Xyr1 (xylanase regulator 1) regulates both the hydrolytic enzyme system and D-xylose metabolism in *Hypocrea jecorina*. *Eukaryot. Cell* **2006**, *5*, 2128–2137. [[CrossRef](#)] [[PubMed](#)]
13. Ilmén, M.; Thrane, C.; Penttilä, M. The glucose repressor gene cre1 of *Trichoderma* isolation and expression of a full-length and a truncated mutant form. *Mol. Gen. Genet.* **1996**, *251*, 451–460. [[PubMed](#)]
14. Häkkinen, M.; Valkonen, M.J.; Westerholm-Parvinen, A.; Aro, N.; Arvas, M.; Vitikainen, M. Screening of candidate regulators for cellulase and hemicellulase production in *Trichoderma reesei* and identification of a factor essential for cellulase production. *Biotechnol. Biofuels* **2014**, *7*, 14–34. [[CrossRef](#)]
15. Karimi Aghcheh, R.; Nemeth, Z.; Atanasova, L.; Fekete, E.; Paholcsek, M.; Sandor, E.; Aquino, B.; Druzhinina, I.S.; Karaffa, L.; Kubicek, C.P. The VELVET A orthologue VEL1 of *Trichoderma reesei* regulates fungal development and is essential for cellulase gene expression. *PLoS ONE* **2014**, *9*, e112799. [[CrossRef](#)]
16. Nitta, M.; Furukawa, T.; Shida, Y.; Mori, K.; Kuhara, S.; Morikawa, Y.; Ogasawara, W. A new Zn(II)(2)Cys(6)-type transcription factor BglR regulates beta-glucosidase expression in *Trichoderma reesei*. *Fungal Genet. Biol.* **2012**, *49*, 388–397. [[CrossRef](#)]
17. Ivanova, C.; Ramoni, J.; Aouam, T.; Frischmann, A.; Seiboth, B.; Baker, S.E.; Le Crom, S.; Lemoine, S.; Margeot, A.; Bidard, F. Genome sequencing and transcriptome analysis of *Trichoderma reesei* QM9978 strain reveals a distal chromosome translocation to be responsible for loss of vib1 expression and loss of cellulase induction. *Biotechnol. Biofuels* **2017**, *10*, 209. [[CrossRef](#)]
18. Zhang, F.; Zhao, X.Q.; Bai, F.W. Improvement of cellulase production in *Trichoderma reesei* Rut-C30 by overexpression of a novel regulatory gene Trvib-1. *Bioresour. Technol.* **2018**, *247*, 676–683. [[CrossRef](#)]
19. Antonieto, A.C.C.; Nogueira, K.M.V.; de Paula, R.G.; Nora, L.C.; Cassiano, M.H.A.; Guaz Zaroni, M.E.; Almeida, F.; da Silva, T.A.; Ries, L.N.A.; de Assis, L.J.; et al. A novel Cys2His2 zinc finger homolog of AZF1 modulates holocellulase expression in *Trichoderma reesei*. *mSystems* **2019**, *4*, e00161-19. [[CrossRef](#)]
20. Cao, Y.L.; Zheng, F.L.; Wang, L.; Zhao, G.L.; Chen, G.J.; Zhang, W.X.; Liu, W.F. Rce1, a novel transcriptional repressor, regulates cellulase gene expression by antagonizing the transactivator Xyr1 in *Trichoderma reesei*. *Mol. Microbiol.* **2017**, *105*, 65–83. [[CrossRef](#)] [[PubMed](#)]
21. Xu, L.Z.; Ajimura, M.; Padmore, R.; Klein, C.; Kleckner, N. NDT80, a meiosis-specific gene required for exit from pachytene in *Saccharomyces cerevisiae*. *Mol. Cell Biol.* **2005**, *15*, 6572–6581. [[CrossRef](#)]
22. Nobile, C.J.; Fox, E.P.; Nett, J.E.; Sorrells, T.R.; Mitrovich, Q.M.; Hernday, A.D.; Tuch, B.B.; Andes, D.R.; Johnson, A.D. A recently evolved transcriptional network controls biofilm development in *Candida albicans*. *Cell* **2012**, *148*, 126–138. [[CrossRef](#)]
23. Katz, M.E.; Braunberger, K.; Yi, G.; Cooper, S.; Nonhebel, H.M.; Gondro, C. A p53-like transcription factor similar to Ndt80 controls the response to nutrient stress in the filamentous fungus, *Aspergillus nidulans*. *F1000Research* **2013**, *2*, 72. [[CrossRef](#)] [[PubMed](#)]
24. Dementhon, K.; Iyer, G.; Glass, N.L. VIB-1 is required for expression of genes necessary for programmed cell death in *Neurospora crassa*. *Eukaryot. Cell* **2006**, *5*, 2161–2173. [[CrossRef](#)]
25. Xiong, Y.; Sun, J.; Glass, N.L. VIB1, a link between glucose signaling and carbon catabolite repression, is essential for plant cell wall degradation by *Neurospora crassa*. *PLoS Genet.* **2014**, *10*, e1004500. [[CrossRef](#)]
26. Verbeke, J.; Coutinho, P.; Mathis, H.; Quenot, A.; Record, E.; Asther, M.; Heiss-Blanquet, S. Transcriptional profiling of cellulase and expansin-related genes in a hypercellulolytic *Trichoderma reesei*. *Biotechnol. Lett.* **2009**, *31*, 1399–1405. [[CrossRef](#)] [[PubMed](#)]
27. Ghose, T.K. Measurement of cellulase activities. *Pure App. Chem.* **1987**, *59*, 257–268. [[CrossRef](#)]



28. Anders, S.; Pyl, P.T.; Huber, W. HTSeq—A Python framework to work with high-throughput sequencing data. *Bioinformatics* **2015**, *31*, 166–169. [[CrossRef](#)] [[PubMed](#)]
29. Schuster, A.; Tisch, D.; Seidl-Seiboth, V.; Kubicek, C.P.; Schmoll, M. Roles of protein kinase A and adenylate cyclase in light-modulated cellulase regulation in *Trichoderma reesei*. *Appl. Environ. Microbiol.* **2012**, *78*, 2168–2178. [[CrossRef](#)] [[PubMed](#)]
30. Chen, X.Z.; Luo, Y.F.; Yu, H.T.; Sun, Y.H.; Wu, H.; Song, S.H.; Hu, S.N.; Dong, Z.Y. Transcriptional profiling of biomass degradation-related genes during *Trichoderma reesei* growth on different carbon sources. *J. Biotechnol.* **2014**, *173*, 59–64. [[CrossRef](#)]
31. Landowski, C.P.; Huuskonen, A.; Wahl, R.; Westerholm-Parvinen, A.; Kanerva, A.; Hanninen, A.L.; Salovuori, N.; Penttila, M.; Natunen, J.; Ostermeier, C.; et al. Enabling low cost biopharmaceuticals: A systematic approach to delete proteases from a well-known protein production host *Trichoderma reesei*. *PLoS ONE* **2015**, *10*, e0134723. [[CrossRef](#)]
32. Ivanova, C.; Baath, J.A.; Seiboth, B.; Kubicek, C.P. Systems analysis of lactose metabolism in *Trichoderma reesei* identifies a lactose permease that is essential for cellulase induction. *PLoS ONE* **2013**, *8*, e62631.
33. Tisch, D.; Kubicek, C.P.; Schmoll, M. The phosphatidylinositol 3-kinase-like protein PhLP1 impacts regulation of glycoside hydrolases and light response in *Trichoderma reesei*. *BMC Genomics* **2011**, *12*, 613. [[CrossRef](#)]
34. Zhang, W.X.; Kou, Y.B.; Xu, J.T.; Cao, Y.L.; Zhao, G.L.; Shao, J.; Wang, H.; Wang, Z.X.; Bao, X.M.; Chen, G.J.; et al. Two major facilitator superfamily sugar transporters from *Trichoderma reesei* and their roles in induction of cellulase biosynthesis. *J. Biol. Chem.* **2013**, *288*, 32861–32872. [[CrossRef](#)] [[PubMed](#)]
35. Nogueira, K.M.V.; de Paula, R.G.; Antonieto, A.C.C.; Dos Reis, T.F.; Carraro, C.B.; Silva, A.C.; Almeida, F.; Rechia, C.G.V.; Goldman, G.H.; Silva, R.N. Characterization of a novel sugar transporter involved in sugarcane bagasse degradation in *Trichoderma reesei*. *Biotechnol. Biofuels* **2018**, *11*, 84. [[CrossRef](#)] [[PubMed](#)]
36. Derntl, C.; Guzman-Chavez, F.; Mello-de-Sousa, T.M.; Busse, H.J.; Driessen, A.J.M.; Mach, R.L.; Mach-Aigner, A.R. In vivo study of the sorbicillinoid gene cluster in *Trichoderma reesei*. *Front. Microbiol.* **2017**, *8*, 2037. [[CrossRef](#)] [[PubMed](#)]
37. Derntl, C.; Kluger, B.; Bueschl, C.; Schuhmacher, R.; Mach, R.L.; Mach-Aigner, A.R. Transcription factor Xpp1 is a switch between primary and secondary fungal metabolism. *Proc. Natl. Acad. Sci. USA* **2017**, *114*, E560–E569. [[CrossRef](#)]
38. Li, C.C.; Lin, F.M.; Sun, W.; Yuan, S.X.; Zhou, Z.H.; Wu, F.G.; Chen, Z. Constitutive hyperproduction of sorbicillinoids in *Trichoderma reesei* ZC121. *Biotechnol. Biofuels* **2018**, *11*, 291. [[CrossRef](#)]
39. Abe, N.; Arakawa, T.; Hirota, A. The biosynthesis of bisvertinolone: Evidence for oxosorbicillinol as a direct precursor. *Chem. Commun.* **2002**, 204–205. [[CrossRef](#)] [[PubMed](#)]
40. Meng, J.J.; Wang, X.H.; Xu, D.; Fu, X.X.; Zhang, X.P.; Lai, D.W.; Zhou, L.G.; Zhang, G.Z. Sorbicillinoids from fungi and their bioactivities. *Molecules* **2016**, *21*, 715. [[CrossRef](#)] [[PubMed](#)]
41. Derntl, C.; Rassinger, A.; Srebotnik, E.; Mach, R.L.; Mach-Aigner, A.R. Identification of the main regulator responsible for synthesis of the typical yellow pigment produced by *Trichoderma reesei*. *Appl. Environ. Microbiol.* **2016**, *82*, 6247–6257. [[CrossRef](#)]
42. Coradetti, S.T.; Craig, J.P.; Xiong, Y.; Shock, T.; Tian, C.G.; Glass, N.L. Conserved and essential transcription factors for cellulase gene expression in ascomycete fungi. *Proc. Natl. Acad. Sci. USA* **2012**, *109*, 7397–7402. [[CrossRef](#)]
43. Kunitake, E.; Kobayashi, T. Conservation and diversity of the regulators of cellulolytic enzyme genes in Ascomycete fungi. *Curr. Genet.* **2017**, *63*, 951–958. [[CrossRef](#)] [[PubMed](#)]
44. Karimi-Aghcheh, R.; Bok, J.W.; Phatale, P.A.; Smith, K.M.; Baker, S.E.; Lichius, A.; Omann, M.; Zeilinger, S.; Seiboth, B.; Rhee, C.; et al. Functional analyses of *Trichoderma reesei* LAE1 reveal conserved and contrasting roles of this regulator. *G3-Genes Genom. Genet.* **2013**, *3*, 369–378.
45. Monroy, A.A.; Stappler, E.; Schuster, A.; Sulyok, M.; Schmoll, M. A CRE1- regulated cluster is responsible for light dependent production of dihydrotrichotetronin in *Trichoderma reesei*. *PLoS ONE* **2017**, *12*, e0182530. [[CrossRef](#)]
46. Hitzenthaler, E.; Buschl, C.; Sulyok, M.; Schuhmacher, R.; Kluger, B.; Wischnitzki, E.; Schmoll, M. YPR2 is a regulator of light modulated carbon and secondary metabolism in *Trichoderma reesei*. *BMC Genom.* **2019**, *20*, 211. [[CrossRef](#)] [[PubMed](#)]
47. Hinterdobler, W.; Schuster, A.; Tisch, D.; Ozkan, E.; Bazafkan, H.; Schinnerl, J.; Brecker, L.; Bohmdorfer, S.; Schmoll, M. The role of PKAc1 in gene regulation and trichodimerol production in *Trichoderma reesei*. *Fungal Biol. Biotechnol.* **2019**, *6*, 12. [[CrossRef](#)] [[PubMed](#)]
48. Beier, S.; Hinterdobler, W.; Bazafkan, H.; Schillinger, L.; Schmoll, M. CLR1 and CLR2 are light dependent regulators of xylanase and pectinase genes in *Trichoderma reesei*. *Fungal Genet. Biol.* **2020**, *136*, 103315. [[CrossRef](#)] [[PubMed](#)]